Marsh, D., Watts, A., & Knowles, P. F. (1976) *Biochemistry 15*, 3570–3578.
Mitaku, S., Ikegami, A., & Sakanishi, A. (1978) *Biophys. Chem. 8*, 295–304.
Mouritsen, O. G., & Bloom, M. (1984) *Biophys. J. 46*, 141–153.
Nagle, J. F., & Scott, H. L. (1978) *Biochim. Biophys. Acta 513*, 236–243.
Neumcke, B., & Läuger, P. (1969) *Biophys. J. 9*, 1160–1170.
Papahadjopoulos, D., Jacobson, K., Nir, S., & Isac, T. (1973) *Biochim. Biophys. Acta 311*, 330–348.
Ralston, E., Hjelmeland, L. M., Klausner, R. D., Weinstein, J. N., & Blumenthal, R. (1981) *Biochim. Biophys. Acta 649*, 133–137.
Schell, R. E., Stevens, B. R., & Wright, E. M. (1983) *J. Physiol. (London) 335*, 307–318.
Thomas, J. A., Buchsbaum, R. N., Zimniak, A., & Racker, E. (1979) *Biochemistry 18*, 2210–2218.
Träuble, H. (1971) *J. Membr. Biol. 4*, 193–209.
Vodyanoy, I., & Hall, J. E. (1984) *Biophys. J. 46*, 187–194.
Watts, A., Marsh, D., & Knowles, P. F. (1978) *Biochemistry 17*, 1792–1801.
Weinstein, J. N., Yoshikami, S., Henkart, P., Blumenthal, R., & Hagins, W. A. (1977) *Science (Washington, D.C.) 195*, 489–492.
Wright, S. H., Krasne, S., Kippen, I., & Wright, E. M. (1981) *Biochim. Biophys. Acta 640*, 767–778.

Influence of Immune Complexes on Macrophage Membrane Fluidity: A Nanosecond Fluorescence Anisotropy Study†

Howard R. Petty,* Charles D. Niebylski, and Joseph W. Francis
Department of Biological Sciences, Wayne State University, Detroit, Michigan 48202
Received October 24, 1986; Revised Manuscript Received May 29, 1987

ABSTRACT: Time-resolved fluorescence anisotropy (TRFA) and steady-state anisotropy measurements and fluorescence intensification microscopic observations were made on RAW264 macrophages labeled with 1,6-diphenyl-1,3,5-hexatriene (DPH) or 1-[4-(trimethylammonio)phenyl]-6-phenyl-1,3,5-hexatriene (TMA-DPH). Microscopic analysis revealed that the fluorescent probe DPH was found in association with plasma membranes and small vesicles. Macrophages treated with immune complexes could not be distinguished from untreated cells, indicating that the same membrane compartments were labeled. The probe TMA-DPH was exclusively localized to the plasma membrane. Steady-state anisotropy measurements indicated that in vitro culture conditions did not significantly affect membrane fluidity. TRFA measurements were conducted to determine the physical properties of macrophage membranes during immune recognition and endocytosis. Data were analyzed by iterative deconvolution to yield ϕ, the rotational correlation time, and r_∞, the limiting anisotropy. These parameters may be interpreted as the "fluidity" and order parameter of the membrane environment, respectively. Typical values for untreated macrophages were ϕ = 7.8 ns and r_∞ = 0.12. Binding and endocytosis of immune complexes prepared in 4-fold antigen excess increase these values to ϕ = 22.1 ns and r_∞ = 0.15. However, receptor-independent phagocytosis of latex beads decreases these values to ϕ = 2.2 ns and r_∞ = 0.10. Addition of catalase before, but not after, immune complex incubation with cells diminishes the effect upon membrane structure, suggesting that H_2O_2 participates in fluidity changes. Pretreatment of macrophages with the membrane-impermeable sulfhydryl blocker *p*-(chloromercuri)benzenesulfonic acid also diminished these effects. Cell-free and immune complex free supernatants of immune complex treated macrophages can decrease the fluidity of resting macrophages. Arachidonic acid at 10 μM increased membrane fluidity while prostaglandin E2 at 10 nM decreased fluidity. Our results indicate an important role of oxidizing agents, sulfhydryl residues, and soluble factors in controlling macrophage membrane fluidity during immune recognition. These factors may account for as much as 98% of the change induced by immune complexes.

The macrophage cell surface is a crucial interface linking molecular immune recognition to the triggering of effector functions. Antibody-dependent recognition triggers a broad spectrum of cellular responses including phagocytosis, cytolysis, release of lysosomal enzymes and mediators such as prostaglandin E2, and release of reactive oxygen metabolites. The molecular membrane events surrounding these functional changes are just beginning to be understood. Murine macrophages possess at least two distinct cell surface receptors for the Fc domain of IgG; FcR2a[1] is specific for IgG2a while FcR2b binds IgG2b (Unkeless, 1977). In the case of IgG2b recognition, the CH2 region of the Fc domain interacts with the FcR2b (Diamond et al., 1985). The IgG2b receptor is a M_r 50 000 glycoprotein (Mellman & Unkeless, 1980). Upon

†This work has been supported by NSF Grant PCM-8207838, by NSF Biological Instrumentation Grant PCM-8313893, and by a grant from the Children's Leukemia Foundation of Michigan.

[1] Abbreviations: DPH, 1,6-diphenyl-1,3,5-hexatriene; TMA-DPH, 1-[4-(trimethylammonio)phenyl]-6-phenyl-1,3,5-hexatriene; TRFA, time-resolved fluorescence anisotropy; db-cAMP, N^6,2′-*O*-dibutyryladenosine cyclic 3′,5′-phosphate; FcR2a, Fc receptor for IgG2a; FcR2b, Fc receptor for IgG2b; PCMBSA, *p*-(chloromercuri)benzenesulfonic acid; HBSS, Hank's balanced salt solution; PBS, phosphate-buffered saline; EDTA, ethylenediaminetetraacetic acid; BSA, bovine serum albumin; DMPC, dimyristoylphosphatidylcholine.

0006-2960/87/0426-6340$01.50/0

ligand binding, the FcR2b can function as an ion channel (Young et al., 1983). Furthermore, an FcR2b-associated phospholipase A2 activity may initiate arachidonic acid metabolism (Suzuki et al., 1982). Jones et al. (1985) have provided evidence indicating that endocytic triggering requires multimeric ligand–receptor interactions. Recently, we have stressed that some of the diverse physiological observables may be explained by a sulfhydryl redox model (Petty, 1985). In particular, a cell surface M_r 25 000 protein, which is precipitated by anti-Fc receptor antibody (Petty, 1987), possesses free cell surface sulfhydryl residues. Oxidative cross-linking of these proteins at the cell surface may account for the unique protein composition of plasma membrane in the vicinity of immune complexes (Petty & Dereski, 1985) and the specific inhibition of FcR-dependent endocytosis mediated by membrane-impermeable sulfhydryl reagents (Dereski & Petty, 1985; H. R. Petty, unpublished results). Furthermore, plasma membrane specializations in the region of antibody-dependent recognition have been previously observed with electron microscopy (Douglas & Huber, 1972; Montesano et al., 1983; Aggeler & Werb, 1982). Alterations in the thickness of the macrophage glycocalyx have also been observed (Richards & Douglas, 1983). The potential oxidative receptor–receptor or receptor–ligand interactions predicted (Petty, 1985) may constitute a molecular mechanistic pathway of the zipper mechanism of phagocytosis (Griffin et al., 1976).

One approach to examining the highly complex and interactive chemical signaling during endocytosis is to measure a physical property of the membrane which is affected by endocytosis. The physical property of membrane fluidity has been frequently invoked to explain functional alterations in membranes (Shinitzky, 1984). In the present report, we study the membrane fluidity of macrophages in response to phagocytic targets and soluble mediators associated with phagocytosis. The techniques of time-resolved and steady-state fluorescence anisotropy and fluorescence intensification microscopy have been utilized to measure rotational correlation times and limiting anisotropies of membrane-intercalated probes. This approach allows for the amelioration of certain limitations of previous fluidity studies. We have quantitated the influences of phagocytosis and mediator interactions upon the dynamic and static properties of macrophage membranes.

Materials and Methods

Cell Culture. The murine macrophage cell line RAW264 was employed in these studies (Raschke et al., 1978). The RAW264 cell line was grown as adherent cells in RPMI1640 medium (Gibco, Grand Island, NY) containing 8% fetal calf serum (Calbiochem, San Diego, CA) and 10 μg/mL penicillin–stretomycin (Gibco). The RAW264 macrophages were removed from tissue culture flasks by incubation for 15–30 min with Hank's balanced salt solution (HBSS) without Ca^{2+} or Mg^{2+} containing 2 mM EDTA. The cells were then washed twice with PBS or HBSS containing Ca^{2+}, Mg^{2+}, and glucose.

Target Particles. Immune complexes were prepared as previously described (Petty & Dereski, 1985). Briefly, rabbit anti-horse ferritin IgG was fractionated by affinity chromatography on columns containing protein A–Sepharose 4B (Pharmacia, Pitscataway, NJ). Immune complexes were formed in 4-fold antigen excess.

Latex beads were prepared and incubated with macrophages are previously described (Petty et al., 1980). Beads of 1.0-μm diameter were obtained from Sigma Chemical Co.

Incubations. Immune complex binding was initiated by addition of 10 μL of ferritin–anti-ferritin at 5 mg/mL to 1 mL of cells at 4×10^5/mL. After incubation at 37 °C for 30 min, cells were washed by centrifugation followed by resuspension in buffer. In some experiments, catalase (Sigma Chemical Co.) was added simultaneously with immune complexes or 2 h later (temporal control) at 1600 units/mL. The membrane-impermeable sulfhydryl reagent *p*-(chloromercuri)benzenesulfonic acid (PCMBSA; Sigma Chemical Co.) was dissolved in PBS at 5 mM and stored in a light-tight container. Macrophages were treated with 0.1–1.0 mM PCMBSA for 30 min at 37 °C before or after immune complex treatment. Cells were also tested with 10 nM prostaglandin E2, 10 μM arachidonic acid, or 30 μM db-cAMP.

Preparation of Mediator Supernatants. Supernatants from immune complex treated macrophages were prepared to test for the presence of soluble factors possessing the ability to alter membrane fluidity. Macrophages in RPMI1640 were treated with immune complexes for 30 min at 4 °C. The cells were washed twice by centrifugation to remove unbound complexes. Cells were then incubated at 37 °C for 1 h. The cell-free supernatant was collected by centrifugation. Untreated cells were incubated in supernate at 37 °C for 30 min. Cells were processed in a fashion identical with that used in the above DPH experiments. Controls were performed with cells not exposed to active supernatants.

Fluorescence Labeling. The fluorescent probes DPH and TMA-DPH were obtained from Molecular Probes, Inc. (Junction City, OR). Reagents were stored frozen in a desiccator. Stock solutions of DPH and TMA-DPH at 1 mM were prepared in tetrahydrofuran and dimethylformamide, respectively. Stock solutions were prepared every 2–3 months and stored at 4 °C until use. An aliquot of a stock solution was diluted 500-fold into PBS followed by shaking for 30 min at room temperature. DPH or TMA-DPH was then added to cells at a final concentration of 0.50 μM. The fluorescent probes were added to cell suspensions following incubation with the target particles, reagents, mediators, or controls as indicated in the text. Measurements were performed at 2×10^5 cells/mL. The effect of light scattering was not significant at this cell concentration.

Fluorescence Microscopy. Cells were examined in a Zeiss fluorescence microscope equipped with special detection instrumentation (Petty & Francis, 1985). A mercury vapor lamp was used for excitation. A Leitz 50× (numerical aperature = 1.0) or 100× (numerical aperature = 1.2) water immersion objective was employed. The image was reflected onto an RCA silicon intensifier tube held in a Dage-MIT Model 65 camera. Video signals were recorded on a Panasonic NV-8050 high-resolution video recorder and displayed on an Audiotronics monitor. Photographs were taken from the screen with a Polaroid camera.

Steady-State Fluorescence Measurements. The steady-state fluorescence measurements were conducted with a Perkin-Elmer (Norwalk, CT) MPF-66 fluorometer linked to a Perkin-Elmer Model 7300 computer utilizing PECLS-III software. For steady-state anisotropy measurements, a polarization attachment was employed to select the horizontal (H) or vertical (V) components of both excitation and emission light. The steady-state anisotropy (r_{ss}) is

$$r = \frac{I_{VV} - I_{VH}G}{I_{VV} + 2I_{VH}G} \quad (1)$$

where I represents the measured intensities. The correction factor G is I_{HV}/I_{HH}; it corrects for the unequal transmission by the optics. Data were acquired by computer for 5 s at each of the polarizer settings to minimize potential photoisomerization of DPH.

Time-Resolved Fluorescence Anisotropy. The theory and methods employed in TRFA have been previously described (Badea & Brand, 1979; Yguerabide, 1972). TRFA was measured by the single photon counting technique using a Photochemical Research Associates (PRA; London, Ontario, Canada) system 3000-ns fluorometer. Excitation was provided by a thyratron-gated PRA Model 510C lamp containing 75–85 kPa of N_2 operating at 30 kHz with a 3.5–4.0-kV potential. The 377-nm N_2 emission line was selected by a grated monochromator and used to excite DPH and TMA-DPH. Pulse width (full width at half-maximum) was 2.0–2.5 ns. Emission data were collected at 430 nm. Scattering was ≤3% for all samples. Data were acquired at ≤2% of the lamp repetition rate. Data containing (4–9) × 10^3 peak channel counts and a 10^3-fold decay were collected in 512 channels using a multichannel analyzer. Samples were maintained at a constant temperature as given below with a circulating water bath. For each sample decay curve, a corresponding lamp profile using a scattering solution (latex beads, milk, and/or unlabeled macrophages) was collected. Experiments utilized a Glan-Thompson cell for selecting polarization of the excitation light and a Polaroid sheat for selecting emission light.

Data Analysis. The time dependence of the fluorescence anisotropy, $r(t)$, is given by

$$r(t) = \frac{I_{VV}(t) - I_{HV}(t)Q}{I_{VV}(t) + 2I_{HV}(t)Q} = \frac{d(t)}{s(t)} \quad (2)$$

where $d(t)$ is the difference curve and $s(t)$ is the sum curve. This equation follows the formalism developed by Chen et al. (1977). Q is a total scaling factor which corrects for differences in excitation light intensity with polarizer orientations and variations in the number of photons per pulse emanating from the flashlamp during the time course of the experiment. This factor is

$$Q = GKI_{cr} \quad (3)$$

where $G = I_{VH}/I_{HH}$ and $K = I_{HV}/I_{VV}$. Both G and K are evaluated during short periods of time when lamp intensity should be constant. The factor I_{cr} is the integrated count ratio; the total number of counts for each curve $[I_{VV}(t)/I_{HV}(t)]$ are obtained. Both the experimental $d(t)$ and $s(t)$ decay curves were corrected for the time-dependent instrument response function. The parameters describing the time-dependent emission anisotropy decay were obtained by deconvolution of the difference curve data. The deconvolution is obtained from analysis of the difference curve for a known representation of the sum curve and an unknown set of parameters defining $r(t)$:

$$d(t) = s(t)r(t) \quad (4)$$

where

$$s(t) = \sum_{i=1}^{n} \alpha_i \exp(-t/\tau_i) \quad (5)$$

and

$$r(t) = \sum_{j=1}^{m} \beta_i \exp(-t/\phi_i) \quad (6)$$

The values of α_i and β_i are the calculated preexponential factors of $s(t)$ and $r(t)$, respectively, τ is the excited-state lifetime, and ϕ is the rotational correlation time. Unless otherwise indicated, the value of ϕ corresponds to $j = 1$ in eq 6. In general, $\beta_1 = r_0 - r_\infty$ where r_∞ is the limiting anisotropy.

The order parameter, S, was calculated from measured values of r according to the relation

$$S^2 = r_\infty/r_0 \quad (7)$$

S reflects the local lipid chain order in membranes. Given the model of Kinosita et al. (1977), this is related to the wobbling motion of DPH within a cone whose central axis is perpenticular to the membrane surface. The maximum value of r_0 measured in the present study for macrophage membranes is 0.365. This is in good agreement with previously measured or calculated values of r_0 (Shinitzky & Barenholtz, 1974). Due to experimental uncertainties in measuring anisotropy at zero time, this value is used for all calculations.

Data were also analyzed according to the relative changes in ϕ or S. The values of % $\Delta\phi$ were calculated as

$$\% \Delta\phi = 100\frac{\phi_{experimental} - \phi_{control}}{\phi_{control}} \quad (8)$$

where the experimental and control values of ϕ are as indicated. The values of % ΔS were calculated in a similar fashion. This approach was previously described by Kury and McConnell (1975).

Interpretation of Data Using "Microviscosity" Formalism. Many workers have interpreted polarization or anisotropy data in terms of membrane microviscosity, η. Some authors have erroneously reported these interpretations as resùlts. The Perrin equation may be used to calculate η_1:

$$\frac{r_0}{r_{ss}} - 1 = Cr\frac{T\tau}{\eta_1} \quad (9)$$

where T is the absolute temperature and Cr is the molecular shape parameter. The subscripts are used to indicate the methods of calculation. For DPH, the value of Cr is (8.6 ± 0.4) × 10^5 P/(deg·s) (Shintzky & Inbar, 1974). The value of η_2 was also determined from the relationship

$$\eta_2 = \phi CrT \quad (10)$$

using time-resolved data. The value of the microviscosity found for a particular cell and fluorophore should be independent of the method and assumptions used to arrive at that value. In cell membranes, we have generally found that η_1 and η_2 are not equivalent. The values of the microviscosities calculated in this study are useful for comparison to earlier studies and in studying membrane structure–function correlations.

Results

Localization of DPH and TMA-DPH in Intact Cells. The experiments presented in this report employ the fluorescent probes DPH and TMA-DPH. To provide information regarding the cellular localization of these probes, we have employed the technique of fluorescence intensification microscopy. In Figure 1, we show fluorescence photomicrographs of labeled RAW264 macrophages. Panels a and b show DPH-labeled cells. As panel a shows, fluorescence was found in association with the periphery of the cell including a vesicular compartment and the plasma membrane. Although the vesicles appear to be labeled at a high density, the relative contributions of the labeled membranes to $r(t)$ are uncertain since microscopic intensities are not corrected for the total membrane area. Therefore, data obtained from the DPH anisotropy measurements reflect the combined properties of at least two membrane compartments. It should be noted from these data that several membrane compartments such as the nuclear and mitochondrial membranes were not labeled. This observation is most simply explained by the physical absence of the probe from these membranes. RAW264 macrophages were treated with a large excess of immune complexes formed in 4-fold antigen excess. The DPH labeling profile of the cells was not changed (Figure 1, panel b), although binding and endocytosis

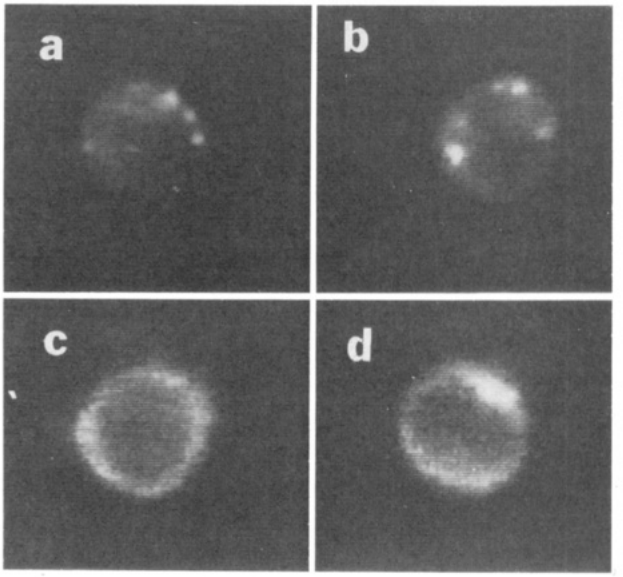

FIGURE 1: Representative fluorescence photomicrographs of DPH- and TMA-DPH-labeled RAW264 macrophages. Panels a and b show DPH-labeled cells whereas panels c and d show TMA-DPH-labeled cells. Panels a and c show untreated cells. Panels b and d show cells treated with immune complexes. Immune complexes do not alter the cellular distribution of these fluorescent probes. All photomicrographs are at a magnification of 1080×.

Table I: Steady-State Fluorescence Anisotropy Studies of Growth Conditions

	r_{ss}	η_1
log phase, media change/day	0.247 ± 0.006	5.10
log phase, media change/3 days	0.240 ± 0.013	4.68
confluent, media change/day	0.246 ± 0.004	5.04
confluent, media change/3 days	0.253 ± 0.003	5.50
overgrown, media change/day	0.244 ± 0.007	4.91
overgrown, media change/3 days	0.254 ± 0.005	5.58

of complexes had taken place. These data indicate that (1) plasma membrane and intracellular vesicles are labeled by DPH and (2) upon interaction with immune complex ligands the intracellular distribution of fluorescent DPH does not change. Furthermore, no change in cell morphology was observed upon addition of DPH. Therefore, in the subsequent studies, DPH is likely measuring the physical properties of the same membrane compartments.

The probe TMA-DPH is positively charged (Prentergast et al., 1983) and therefore should only intercalate in the outer leaflet of the plasma membrane. In Figure 1 (panels c and d), we confirm this assertion. The cells of panels c (untreated) and d (immune complex treated) clearly show that labeling is specific for the plasma membrane. This probe provides another useful control for the plasma membrane associated changes in membrane properties.

Steady-State Fluorescence Anisotropy: Influence of Culture Conditions. The use of a macrophage cell line is advantageous in fluorescence studies since other cell types or cell subpopulations do not influence the measurements. However, cell culture conditions must be studied to determine the effects of in vitro growth on membrane fluidity. In Table I, we show steady-state fluorescence anisotropy data of DPH-labeled RAW264 macrophages. Data are shown as mean ± SE of four independent trials of duplicate or quadruplicate measurements. Cell cultures were initiated at appropriate densities to yield log-phase, confluent, or overgrown cultures after 3 days. Tissue culture media were replaced with fresh media every day or every third day. The cells were removed as described above. In these experiments, the mean anisotropy

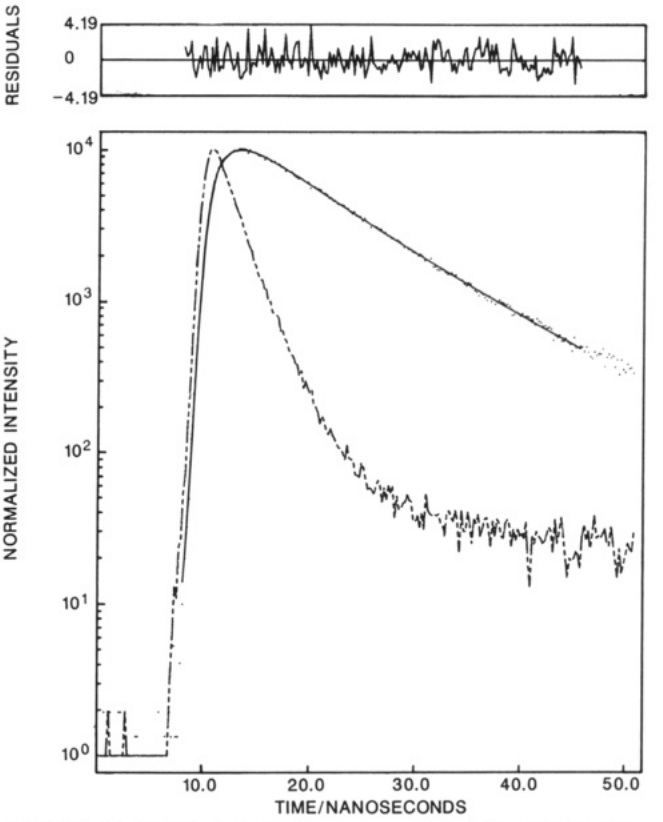

FIGURE 2: Typical fluorescence decay curve of the total emission, $s(t)$, for DPH in macrophage membranes at 20 °C. A semilogarithmic plot of intensity (ordinate) vs. time (abscissa) is given. The lamp curve (- - -), the calculated deconvolution (—), and the experimental data points (•••) are shown. In this example, the values $\alpha_1 = 0.245 \pm 0.008$, $\alpha_2 = 0.108 \pm 0.006$, $\tau_1 = 9.67 \pm 0.12$, and $\tau_2 = 3.16 \pm 0.37$ were found. In this example, the time from 0 to 8 ns was used to accumulate background count rates. They contained no data relevant to cell membranes. Similarly, the following figures also have roughly the initial 8 ns reserved for the background controls. The calculated residuals are shown above the decay curve. The value of χ^2 is 0.901.

value was within the range 0.240–0.253. Day-to-day variability of anisotropy values was most significant for log-phase cells with new media on a 3-day schedule. Therefore, untreated cells have been examined during each experiment to ensure that growth conditions have not affected DPH anisotropy values. Overgrown cells demonstrated the lowest viability (range 92–93.5%) and were therefore avoided. There was no significant effect of culture conditions upon steady-state anisotropy; however, some day-to-day variability was noted.

Time-Resolved Fluorescence Anisotropy. The 337-nm emission line of N_2 was chosen for fluorophore excitation. Although this is slightly removed from the absorption peak, the increased excitation intensity led to greater fluorescence emission in comparison to other N_2 or H_2 lines. Therefore, all data reported employ this condition. Time courses of fluorescence intensity and depolarization of DPH and TMA-DPH in macrophage membranes were measured. The influences of immune complexes, latex beads, chemical probes, and exogenous and endogenous mediators on ϕ and r_∞ of macrophage membranes were investigated. As an example, the fluorescence decay curves $s(t)$ and $d(t)$ of DPH in resting macrophage membranes are shown in Figures 2 and 3, respectively. The data were analyzed as discussed under Materials and Methods. A least-squares algorithm was employed to test the quality of the mathematical analysis to the data points (PRA, Inc.); the residuals for each fit are given in Figures 2 and 3. The χ^2 values were all of an acceptable magnitude.

Table II: Physical Properties of RAW264 Macrophage Membranes[a,b]

treatment	measured quantities: ϕ (ns)[c] mean	measured quantities: r_∞ range	measured quantities: r_∞ mean	calculated quantities: n	calculated quantities: η_2 (P) mean	calculated quantities: S mean
controls	7.0 ± 1.5	0.08–0.12	0.11	15	1.76	0.55
immune complexes	22.1 ± 7.8	0.11–0.19	0.15	7	5.57	0.64
antigen only	8.3 ± 0.8	0.10	0.10	2	2.09	0.52
controls, 30 °C	5.5 ± 1.3	0.07–0.16	0.12	3	1.43	0.57
latex	2.2 ± 0.4	0.08–0.13	0.10	2	0.554	0.52
immune complexes + catalase	11.6 ± 4.1	0.10–0.17	0.14	3	2.92	0.62
immune complexes for 30 min, then catalase	22.5 ± 8.5	0.17–0.21	0.19	2	5.67	0.72
PCMBSA	6.7 ± 2.1	0.11–0.13	0.12	3	1.69	0.57
PCMBSA pretreatment, then immune complexes	9.0 ± 3.6	0.11–0.17	0.13	3	2.27	0.57
immune complexes for 30 min, then PCMBSA	11.7 ± 3.2	0.11–0.15	0.13	2	2.95	0.60
ethanol control	7.6 ± 1.2	0.091–0.11	0.10	3	1.92	0.52
arachidonic acid	3.5 ± 0.5	0.071–0.083	0.076	3	0.882	0.46
prostaglandin E2	13.6 ± 1.5	0.11–0.14	0.12	5	3.43	0.57
db-cAMP	11.1 ± 2.5	0.11–0.12	0.11	4	2.80	0.55
supernatant	15.5 ± 1.4	0.13–0.14	0.13	2	3.80	0.59
supernatant + catalase	11.4 ± 1.5	0.11–0.14	0.13	2	2.87	0.62

[a] All measurements were performed at 20 °C unless otherwise indicated. [b] The quantities employed were as follows: catalase, 1600 units/mL; PCMBSA, 10 mM; arachidonic acid, 10 μM; prostaglandin E2, 10 nM; ethanol, 3.3 × 10^{-4}%; db-cAMP, 30 μM. [c] Mean ± SE.

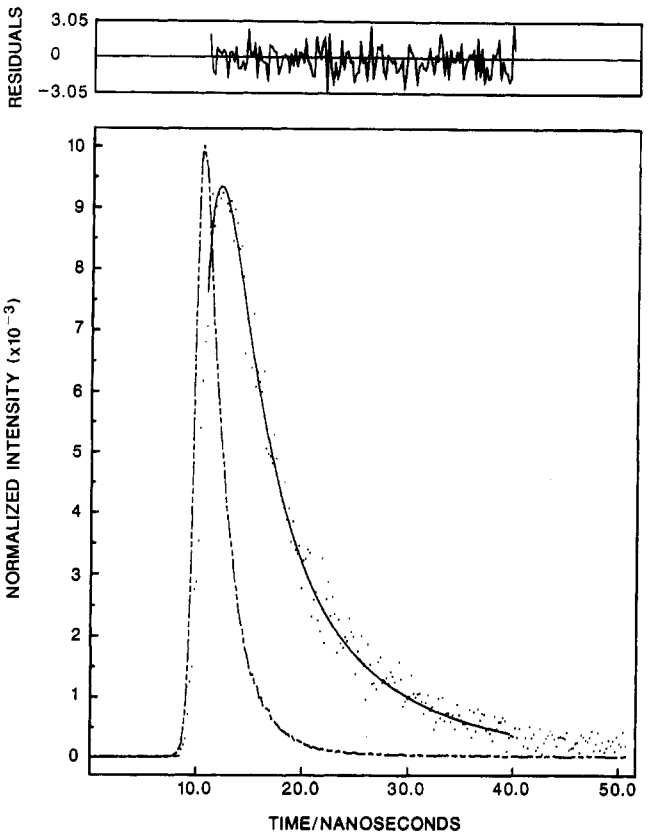

FIGURE 3: Experimental difference curve, $d(t)$, from the same data set as that of Figure 2. The normalized intensity is shown in linear form. The lamp pulse (- - -), difference data anlysis (—), and data points (···) are shown. A plot of the residuals is shown above the figure. The χ^2 value is 0.970.

The viscosity of a medium is a function of temperature. Therefore, it should be possible to confirm the temperature dependence of membrane lipid properties. In Table II are shown data of DPH-labeled macrophages at 20 and 30 °C. The 10 °C increase in temperature significantly decreased the value of ϕ while r_∞ was not affected.

Figure 4 shows a summary of representative time-resolved anisotropy experiments performed with control and treated DPH-labeled macrophages. As mentioned under Materials and Methods, cells were labeled with fluorescent probes after incubation with particles, mediators, or reagents. Each dot represents one datum; the abscissa is time in nanoseconds while

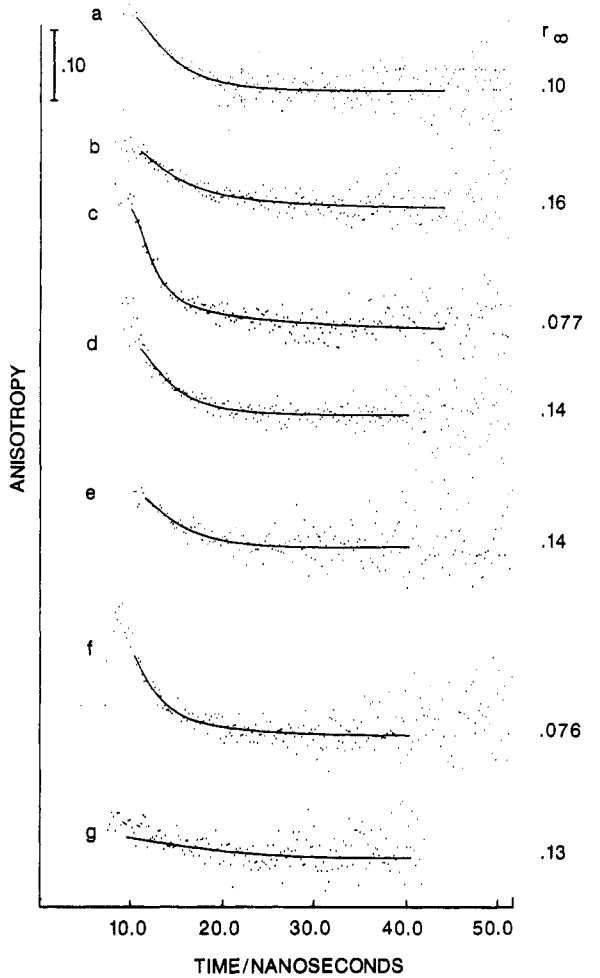

FIGURE 4: Representative time-resolved decays of DPH emission anisotropy in RAW264 macrophages. Both the experimental data points (···) and calculated decay curves (—) are given. The ordinate is the fluorescence emission anisotropy while the abscissa is the time in nanoseconds. The magnitude of 0.10 anisotropy unit is shown at the upper left-hand corner. The values of r_∞ for each decay curve are shown on the right-hand side. The traces show typical examples of macrophages exposed to (a) control conditions, (b) immune complexes, (c) latex beads, (d) PCMBSA and then immune complexes, (e) immune complexes and catalase, (f) 10 μM arachidonic acid, and (g) 10 nM prostaglandin E2. (See text for details and further controls.)

the ordinate is anisotropy. The solid lines are the calculated fit to the anisotropy data. In Figure 4a–c, the values of ϕ and

r_∞ were found to be 6.5 ± 0.4 ns and 0.10 ± 0.01 for control cells, 12.5 ± 1.4 ns and 0.16 ± 0.01 for immune complex treated cells, and 2.6 ± 0.4 ns and 0.08 ± 0.01 for latex bead treated cells. For all studies of macrophages treated in these fashions, the following values were obtained: immune complex treatment, ϕ = 22.1 ± 7.8 ns and r_∞ = 0.15 ± 0.03; control, ϕ = 7.0 ± 1.5 ns and r_∞ = 0.11 ± 0.02; latex bead treatment, ϕ = 2.2 ± 0.4 ns and r_∞ = 0.10 ± 0.01. Incubation of macrophages with antigen alone had no significant effect upon either parameter (Table II). Macrophage membranes become substantially less fluid as indicated by both ϕ and r_∞ after exposure to immune complexes. This central observation was confirmed with steady-state anisotropy measurements. Control and immune complex treated cells yielded r_{ss} values of 0.231 ± 0.006 and 0.279 ± 0.003, respectively. However, latex bead uptake induces a substantial increase in the fluidity of the DPH-labeled membranes.

The values of the standard deviations reported in Table II for all experiments are somewhat larger than those given for a particular data set. This is not due to instrumental inconsistencies but rather due to day-to-day variability in the cells. These small differences may be a manifestation of differences in medium composition [e.g., see Mahoney et al. (1977)] and the cell cycle (Obrenovitch et al., 1978). The values of ϕ, r_∞, η_2, and S reported in Tables I and II for control studies are in good agreement with previous reports (Ricardo et al., 1986; Liebes et al., 1981; Cherenkevich et al., 1982a,b; Larsen et al., 1984; Sandor et al., 1981).

Several experiments were conducted to probe the chemical nature of the immune complex induced decrease in fluidity. We shall consider first the effects of the enzyme catalase, which catalyzes the decomposition of H_2O_2. Simultaneous addition of immune complexes and catalase at 1600 units/mL to macrophages diminishes the effects of immune complexes on membrane fluidity (Figure 4e). There was little or no effect upon the value of r_∞ although ϕ = 11.6 ± 4.1 ns was significantly lower than immune complex treated macrophages (Table II). Using % $\Delta\phi = 100(\Delta\phi/\phi)$ as defined above, we find that catalase-sensitive molecules account for % $\Delta\phi$ = 66 (or a percentile of 31%) of the immune complex induced increase in the rotational correlation time. These effects, however, must be considered as a lower boundary since catalase alone tends to decrease membrane fluidity. Although this effect has been previously observed (Ingrham et al., 1981), its origin is not known. The addition of catalase 2 h after immune complex treatment did not diminish the effect of immune complexes on membrane fluidity (Table II). This indicates a time-dependent effect of H_2O_2 on membranes, as expected.

The contribution of cell surface sulfhydryl groups to fluidity changes was assessed by using the membrane-impermeable sulfhydryl-specific reagent PCMBSA. Pretreatment of RAW264 macrophages with 1.0 mM PCMBSA followed by incubation with immune complexes resulted in little or no increase in ϕ (6.7 ± 2.1 ns) and r_∞ (0.12 ± 0.01). Preincubation of macrophages with PCMBSA diminished the immune complex mediated decrease in fluidity (Figure 4d). Immune complexes increased ϕ to 9.0 ± 3.6 ns and r_∞ to 0.13 ± 0.03. A major portion of the immune complex mediated increase in fluidity can be accounted for by PCMBSA-sensitive sites. The values of ϕ and r_∞ are further increased if immune complexes are added 30 min prior to PCMBSA (Table II). These experiments suggest that PCMBSA inhibits a time-dependent process affecting membrane fluidity. Catalase caused no further change of fluidity in PCMBSA-pretreated macrophages in the presence of immune complexes (ϕ = 9.0 ± 0.9 ns, r_∞ = 0.14).

Table III: Possible Accounting of Membrane Fluidity Changes[a]

contributing factors	% Δφ column A	% Δφ column B	percentile
(1) catalase sensitive (H_2O_2)	66	66	31
(2) catalase insensitive, PCMBSA sensitive	37	37	17
(3) catalase-insensitive soluble mediators	63	63	29
(4) prostaglandin E2	64	64	44
(5) db-cAMP	59	0	0
(6) arachidonic acid	−50	−50	−23
	total 269	210	98
(7) immune complex treatment	216	216	100

[a] PCMBSA blocks certain effects; it is not a mediator. To calculate its contribution, the values of ϕ were treated as [(immune complex + catalase) − (immune complex + PCMBSA + catalase)]/control. This accounts for the PCMBSA contribution beyond that already indicated as catalase sensitive (row 1). Rows 3–6 use macrophages not exposed to immune complexes to determine the contributions of individual mediators.

The possible presence of unidentified mediators released from immune complex treated cells which are capable of influencing membrane fluidity has been tested. Immune complex free supernatants from immune complex treated cells or controls were incubated with native cells at 37 °C for 30 min to 1 h. The mean value of ϕ increased from 7.0 ns in controls to 15.5 ns in supernatant-treated cells. The limiting anisotropy increased from 0.10 to 0.13. Soluble factors can account for a fraction of the observed fluidity changes (Table II). H_2O_2 may be present in the mediator supernatants. As a control for H_2O_2, catalase was added to supernatants prior to cell treatment. In this experiment, the value of ϕ decreased to 11.4 ± 1.5 ns while r_∞ was not significantly changed in comparison to mediator-treated cells. This indicates that H_2O_2 can account for only a portion of the response found with mediator supernatants.

The chemical components contributing to the fluidity changes were further characterized by using defined reagents. Arachidonic acid at 10 μM decreases ϕ (3.5 ± 0.5 ns) and r_∞ (0.076) in comparison to controls (Table II). However, prostaglandin E2 significantly increased ϕ (13.6 ± 1.5 ns) and r_∞ (0.13) at 10 nM. These effects are illustrated in Figure 4f and Figure 4g, respectively. Since ethanol was used as a solvent for these molecules, control studies using ethanol at a final concentration of 3.3×10^{-4}% were performed. As shown in Table II, ethanol at the same concentration as that used in the prostaglandin E2 and arachidonic acid experiments has no significant effect upon the rotational correlation time and limiting anisotropy. Prostaglandin E2 and arachidonic acid produced by immune complex binding have opposing effects on membrane fluidity. In addition to extracellular mediators, intracellular mediators may also influence membrane fluidity. To test this possibility, cells were treated with 30 μM db-cAMP. This concentration of db-cAMP corresponds to the increased intracellular level of cAMP found in phagocytosing macrophages (Seyberth et al., 1973). The values of ϕ and r_∞ in these examples were 8.2 ± 1.3 ns and 0.091 for concurrent measurements of DPH in control macrophages and 15.1 ± 2.5 ns and 0.12 for db-cAMP-treated cells (see also Table III).

To provide an additional control for the participation of the plasma membrane in the observed fluidity changes, the probe TMA-DPH was employed. Due to the positively charged trimethylamino group, this probe becomes localized in the outer leaflet of bilayer membranes (see Figure 1, panels c and

d). Cells were incubated at 37 °C in the absence and presence of immune complexes. No significant change in r_∞ was observed (0.27 ± 0.01 vs. 0.26 ± 0.01). However, ϕ increased from 5.4 ± 1 ns in controls to 8.0 ± 1.2 ns in immune complex treated cells. The immune complex mediated increase in rotational correlation time of TMA-DPH is in qualitative agreement with that of DPH. Quantitative agreement is not expected since these two probes sample different environments. The relatively high values of r_∞ (or equivalently S) indicate substantial hindrance of probe "wobble" or "tilt" (e.g., for TMA-DPH, $r_\infty = 0.26$ whereas $r_\infty = 0.10$ for DPH). This is not surprising since a flexibility gradient within membranes has been previously demonstrated (McConnell, 1976; Hubbell & McConnell, 1971). Therefore, TMA-DPH samples a more ordered environment, as expected due to its location. The increased value of ϕ corroborates the decreased fluidity of the plasma membrane upon exposure to immune complexes.

Discussion

Time-resolved measurements of fluorescence anisotropy decay can be used to determine the rotational motion of molecules embedded within membranes. According to current models of fluorescence depolarization in membranes, both the rate and the angular range of rotational motion can be determined (Kinosita et al., 1979). Computer-aided data analysis can be employed to extract both dynamic (fluidity) and static (order parameter) information regarding probe mobility (Heyn, 1979). In the case of simple model membranes, measurements of the order parameter are a very good indicator of membrane fluidity (Hubbell & McConnell, 1971). In the highly complex membranes of living cells, the correspondence between the rotational correlation time and the order parameter may not be the same. Microviscosity calculations performed with steady-state anisotropy data require several assumptions. Furthermore, interpretation of data obtained from cells is severely limited inasmuch as probe location is frequently unknown. Changes in probe location due to the influence of exogenous or endogenous mediators have not been addressed. Lastly, microviscosity studies are generally of a phenomenological nature; quantitative chemical rationale to account for experimental observations is not often given. In the present report, we have addressed these frequent limitations of fluidity experiments.

Prior investigations on membrane fluidity changes during phagocytosis have presented apparently conflicting results. Berlin and Fera (1977) have reported that membrane microviscosity is decreased significantly after endocytosis of BSA-coated paraffin oil particles and polystyrene beads. On the other hand, Ingraham et al. (1981) and Sandor et al. (1981) have observed increased microviscosity following uptake of opsonized zymosan and immune complexes, respectively. In the present report, we have confirmed all of the above findings. Latex bead uptake decreased membrane microviscosity as indicated by both ϕ and r_∞ while immune complex treatment increased microviscosity. We have similarly observed a decreased fluidity of macrophage membranes after treatment with zymosan (unpublished results). These distinct responses of receptor-independent and receptor-dependent phagocytosis can be accounted for in part by prostaglandin synthesis. Prostaglandin E2, which decreases fluidity, is produced during receptor-mediated but not receptor-independent phagocytosis (Rouzer et al., 1980).

Ingraham et al. (1981) were the first to associate reactive oxygen metabolites with fluidity changes in polymorphonuclear leukocyte membranes. A portion of the effects of H_2O_2 on membrane fluidity may be accounted for by lipid peroxidation (Dobretsov et al., 1977). Although the presence of H_2O_2 affects untreated cells, PCMBSA protects cells from a large portion of these changes. PCMBSA and catalase both diminish the immune complex triggered decrease in fluidity. However, catalase is unable to augment the effect of PCMBSA, suggesting that they are acting on the same pathway. Since PCMBSA is a membrane-impermeable sulfhydryl-specific reagent, cell surface sulfhydryl residues may participate in this pathway. PCMBSA may act upon one or more sites participating in antibody-dependent endocytic recognition and signaling: (1) a membrane protein associated with the FcR2b may be directly modified (H. R. Petty, unpublished results); (2) direct or indirect inhibition of the respiratory burst (Tsan et al., 1976), which may be a requisite for endocytic signaling (Petty, 1985); and/or (3) inhibition of membrane components participating in prostaglandin E2 production (Grundfest et al., 1982). One or more of these interrelated pathways may contribute to the observed effects of PCMBSA on membrane fluidity and its inhibition of membrane fluidity changes caused by mediators.

Chemical mediators released from immune complex treated macrophages are good candidates for agents which may affect membrane fluidity. An unfractionated immune complex free supernatant from immune complex treated macrophages was shown to affect the fluidity of macrophage membranes. Only a fraction of this activity could be destroyed by catalase. Additional long-lived oxidative agents may contribute to the observed fluidity changes (Test et al., 1984).

Upon immune complex binding, macrophages mobilize endogenous stores of arachidonic acid and synthesize prostaglandin (Humes et al., 1977; Rouzer et al., 1980). These compounds are released into the extracellular environment. Since arachidonic acid and prostaglandins have considerable hydrophobic character, they may influence the physical properties of associated bilayers. In the case of prostaglandin E2, specific macrophage cell surface receptors bind this ligand (Opmeer et al., 1983, 1984; Fernandez-Botran & Suzuki, 1984a; Eriksen et al., 1985). In the present study, we have tested the effects of 10 nM prostaglandin E2 and 10 μM arachidonic acid on macrophage membrane fluidity. These doses were chosen because they correspond to typical levels found in in vitro systems employing macrophages and receptor-mediated binding (Friedman et al., 1979; Glatt et al., 1977; Razin et al., 1982; Cantarow et al., 1978; Taffet et al., 1982). Arachidonic acid increased the fluidity and decreased the order parameter of macrophage membranes. These observations are not surprising since it is a polyunsaturated free fatty acid. In contrast, prostaglandin E2 decreases the fluidity and increases the order parameter of RAW264 membranes. The origins of these changes are not certain. One possible factor is specific membrane changes due to the binding of prostaglandin E2 receptors. Another possible factor contributing to the prostaglandin E2 mediated changes is cAMP (see below). The present study has employed rabbit IgG which binds to both the FcR2a and the FcR2b. Nitta and Suzuki (1982b) have reported that the IgG2b but not the IgG2a Fc receptor triggers the release of arachidonic acid and prostaglandins. It would therefore be of interest to test the IgG subclass specificity of the fluidity changes we have observed.

Phagocytosis (Seyberth et al., 1973) and prostaglandin E2 (Gemsa et al., 1975; Fernandez-Botran & Suzuki, 1984b; Eriksen et al., 1985) are known to increase macrophage cAMP levels. The concentration of prostaglandin E2 used in the present study corresponds to the half-maximal stimulation of cAMP in intact cells (Eriksen et al., 1985). The concentration

of db-cAMP, 30 μM, approximates the increased intracellular cAMP levels found during phagocytosis (Seyberth et al., 1973). The cellular volume (Petty et al., 1981) and protein factors (0.23 mg of protein/10^6 cells) were used in this calculation. At a physiologically relevant concentration, the analogue db-cAMP decreases the fluidity of macrophage membranes. Kury and McConnell (1975) have previously observed that cAMP decreases the membrane fluidity of erythrocyte ghosts. The effect of prostaglandin E2 on ϕ may be at least partially accounted for by a change in intracellular cAMP concentration. Furthermore, db-cAMP, which is sufficient to decrease fluidity, decreases phagocytosis of opsonized particles (Goodell et al., 1978).

In Table III, we provide one formulation of the several factors which influence membrane fluidity during receptor-mediated endocytosis. The values of % $\Delta\phi$ were calculated according to eq 6. The percent change in S was not sufficient to quantitatively compare these factors. Qualitatively, the several factors (see Table II) do contribute to an overall change in S. The first column of Table III lists all of the components which may influence macrophage membrane fluidity. The redundancy of H_2O_2 effects is eliminated by adding catalase in the experiments of rows 2 and 3. In column B, the proposed "bookkeeping" of ϕ changes is given. The effects of db-cAMP are deleted because they likely constitute one part of the changes mediated by prostaglandin E2. The total value of % $\Delta\phi$, 210, is near the overall influence of immune complexes, % $\Delta\phi$ = 216. The accounting must be considered as an overestimate since the molecules prostaglandin E2 and arachidonic acid may be present in the preparation of soluble mediators. Since DPH is associated with at least two membrane compartments, the measured responses to the various membrane-impermeable factors may be of an indirect nature. Furthermore, possible compositional changes in the membrane unrelated to the above have not been taken into account (e.g., phospholipid head groups). Nonetheless, a very significant fraction (<98%) of the fluidity changes can be understood in this fashion.

Although the data of Tables II and III quantitatively describe the influence of immune complexes on membrane fluidity, a qualitative idea of what these changes physically represent is not obvious. For purposes of comparison, we consider TRFA measurements using DPH-labeled DMPC liposomes (J. W. Klein, G. Barclay, B. R. Ware, and H. R. Petty, unpublished results). The phase transition temperature of DMPC is 24 °C. At 30 °C, r_∞ = 0.05, S = 0.37, and ϕ = 2.1 ns were found for these liposomes. The values of these parameters at 10 °C were r_∞ = 0.29, S = 0.89, and ϕ = 5.3 ns. The decrease in fluidity can be represented as % $\Delta\phi$ = 152 and % ΔS = 141. Immune complex binding to macrophages yields % $\Delta\phi$ = 216 and % ΔS = 23 (Table II). The diminished fluidity of the macrophage membrane as reflected by ϕ in response to interactions with immune complexes is considerably more dramatic than a phase transition in a model membrane. The change in S is less pronounced, although it clearly indicates a decreased fluidity. The value of S may be interpreted as a relative angular displacement normal to the surface (Kinosita et al., 1979). The heterogenity of cellular membranes may not allow for the lipid–lipid interactions which contribute to the larger range of S found in liposomes.

The observed changes in membrane fluidity may play a role in controlling endocytosis. Previous studies from several laboratories have indicated that membrane fatty acid composition affects endocytosis (Schroit & Gallily, 1979; Mahoney et al., 1977, 1980; Lokesh & Wrann, 1984). Phospholipid head-group composition affects endocytosis in fibroblasts (Schroeder, 1981). These studies have shown that membrane fluidity and content of unsaturated fatty acids directly correlate with the ability of macrophages to pinocytose and phagocytose. Therefore, decreases in membrane fluidity would be expected to down-regulate endocytotic function. Consequently, the depression of membrane fluidity characterized in the present study may provide a down-regulatory mechanism to limit the rate and extent of endocytosis.

ACKNOWLEDGMENTS

We thank K. Berg for her assistance in some of these studies.

Registry No. cAMP, 60-92-4; H_2O_2, 7722-84-1; arachidonic acid, 506-32-1; prostaglandin E2, 363-24-6.

REFERENCES

Aggeler, J., & Werb, Z. (1982) *J. Cell Biol. 94*, 613.
Badea, M. G., & Brand, L. (1979) *Methods Enzymol. 61*, 378.
Berlin, R. D., & Fera, J. P. (1977) *Proc. Natl. Acad. Sci. U.S.A. 74*, 1072.
Cantarow, W. D., Cheung, H. T., & Sundharadas, G. (1978) *Prostaglandins 16*, 39.
Chen, L. A., Dale, R. E., Roth, S., & Brand, L. (1977) *J. Biol. Chem. 252*, 2163.
Cherenkevich, S. N., Vanderkooi, J. M., & Holian, A. (1982a) *Arch. Biochem. Biophys. 214*, 305.
Cherenkevich, S. N., Vanderkooi, J. M., Restifo, R., Daniele, R. P., & Holian, A. (1982b) *Arch. Biochem. Biophys. 214*, 299.
Dale, R. E., Chen, L. A., & Brand, L. (1977) *J. Biol. Chem. 252*, 7500.
Dereski, W., & Petty, H. R. (1985) *Immunology 54*, 397.
Diamond, B., Boccumini, L., & Birshtein, B. K. (1985) *J. Immunol. 134*, 1080.
Dobretsov, G. E., Broschevskaya, T. A., Petrov, V. A., & Vladimirov, Y. A. (1977) *FEBS Lett. 84*, 125.
Douglas, S. D., & Huber, H. (1972) *Exp. Cell Res. 70*, 161.
Engel, L. W., & Prendergast, F. G. (1981) *Biochemistry 20*, 7338.
Eriksen, E. F., Richelsen, B., Beck-Nielsen, H., Melsen, F., Nielsen, H. K., & Mosekide, L. (1985) *Scand. J. Immunol. 21*, 167.
Fernandez-Botran, R., & Suzuki, T. (1984a) *J. Immunol. 133*, 2662.
Fernandez-Botran, R., & Suzuki, T. (1984b) *J. Immunol. 133*, 2655.
Friedman, S. A., Remold-O'Donnell, E., & Piessens, W. F. (1979) *Cell. Immunol. 42*, 213.
Fulford, A. J. C., & Peel, W. E. (1980) *Biochim. Biophys. Acta 598*, 237.
Glatt, M., Kalin, H., Wagner, K., & Brune, K. (1977) *Agents Actions 7*, 321.
Goodell, E. M., Bilgin, S., & Carchman, R. A. (1978) *Exp. Cell Res. 114*, 57.
Griffin, F. A., Griffin, J. A., & Silverstein, S. C. (1976) *J. Exp. Med. 144*, 788.
Grundfest, C. C., Chang, J., & Newcombe, D. (1982) *Biochim. Biophys. Acta 713*, 149.
Haak, R. A., Ingraham, L. M., Baehner, R. L., & Boxer, L. A. (1979) *J. Clin. Invest. 64*, 138.
Heyn, M. P. (1979) *FEBS Lett. 108*, 359.
Hildebrand, K., & Nicolau, C. (1979) *Biochim. Biophys. Acta 553*, 365.
Hubbell, W. L., & McConnell, H. M. (1971) *J. Am. Chem. Soc. 93*, 314.

Ingraham, L. M., Boxer, L. A., Haak, R. A., & Baehner, R. L. (1981) *Blood 58*, 830.
Jones, D. H., Nusbacher, J., & Anderson, C. L. (1985) *J. Cell Biol. 100*, 558.
Kinosita, K., Kawato, S., & Ikegami, A. (1979) *Biophys. J. 20*, 289.
Kury, P. G., & McConnell, H. M. (1975) *Biochemistry 14*, 2798.
Lakowicz, J. R. (1983) *Principles of Fluorescence Spectroscopy*, Plenum Press, New York.
Larsen, N. E., Enelow, R. I., Simons, E. R., & Sullivan, R. (1985) *Biochim. Biophys. Acta 815*, 1.
Liebes, L. F., Pelle, E., Zucker-Franklin, D., & Silber, R. (1980) *Cancer Res. 41*, 4050.
Lokesh, B. R., & Wrann, M. (1984) *Biochim. Biophys. Acta 792*, 141.
Mahoney, E. M., Hamill, A. L., Scott, W. A., & Cohn, Z. A. (1977) *Proc. Natl. Acad. Sci. U.S.A. 74*, 4895.
Mahoney, E. M., Scott, W. A., Landsberger, F. R., Hamill, A. L., & Cohn, Z. A. (1980) *J. Biol. Chem. 255*, 4910.
McConnell, H. M. (1976) in *Spin Labeling: Theory and Applications* (Berliner, L. J., Ed.) p 525, Academic Press, New York.
Mellman, I. A., & Unkeless, J. C. (1980) *J. Exp. Med. 140*, 1287.
Montesano, R., Mossaz, A., Vassalli, P., & Orci, L. (1983) *J. Cell Biol. 96*, 1227.
Nitta, T., & Suzuki, T. (1982a) *J. Immunol. 129*, 2708.
Nitta, T., & Suzuki, T. (1982b) *J. Immunol. 128*, 2527.
Obrenovitch, A., Sene, C., Negre, M. T., & Monsigny, M. (1978) *FEBS Lett. 88*, 187.
Opmeer, F. A., Adolfs, M. J. P., & Bonta, I. L. (1983) *Biochem. Biophys. Res. Commun. 114*, 155.
Opmeer, F. A., Adolfs, M. J. P., & Bonta, I. L. (1984) *J. Lipid Res. 25*, 262.
Petty, H. R. (1985) *Mol. Immunol. 22*, 1001.
Petty, H. R. (1987) *Immunology 60*, 269.
Petty, H. R., & Dereski, W. (1985) *Biochemistry 24*, 4141.
Petty, H. R., & Francis, J. W. (1985) *Biophys. J. 47*, 837.
Petty, H. R., Hafeman, D. G., & McConnell, H. M. (1980) *J. Immunol. 125*, 2391.
Petty, H. R., Hafeman, D. G., & McConnell, H. M. (1981) *J. Cell Biol. 89*, 223.
Prendergast, F. G., Haugland, R. P., & Callahan, P. J. (1981) *Biochemistry 20*, 7333.
Raschke, W. C., Baird, S., Ralph, P., & Nakoinz, I. (1978) *Cell (Cambridge, Mass.) 15*, 261.
Razin, E., Globerson, A., & Skutelsky, E. (1982) *Prostaglandins, Leukotrienes Med. 8*, 301.
Ricardo, M. J., Small, G. W., Myrvik, Q. N., & Kucera, L. S. (1986) *J. Immunol. 136*, 1054.
Richards, K. L., & Douglas, S. D. (1983) *RES: J. Reticuloendothel. Soc. 33*, 305.
Rouzer, C. A., Scott, W. A., Kempe, J., & Cohn, Z. A. (1980) *Proc. Natl. Acad. Sci. U.S.A. 77*, 4279.
Sandor, M., Bagyinka, C., Horvath, L. I., Medgyesi, G. A., Miklos, K., & Gergly, J. (1981) *Mol. Immunol. 18*, 173.
Schroeder, F. (1981) *Biochim. Biophys. Acta 649*, 162.
Schroit, A. J., & Gallily, R. (1979) *Immunology 36*, 199.
Seyberth, H. W., Schmidtgayk, H., Jakobs, K. H., & Hackenthal, E. (1973) *J. Cell Biol. 57*, 567.
Shinitzky, M. (1984) *Physiology of Membrane Fluidity*, Vol. II, CRC Press, Boca Raton, FL.
Shinitzky, M., & Barenholtz, Y. (1974) *J. Biol. Chem. 249*, 2652.
Shinitzky, M., & Inbar, M. (1974) *J. Mol. Biol. 85*, 603.
Stolc, V. (1981) *Mol. Immunol. 18*, 773.
Suzuki, T., Saito-Taki, T., Sadasivan, R., & Nitta, T. (1982) *Proc. Natl. Acad. Sci. U.S.A. 79*, 591.
Taffet, S. M., Eurell, T. E., & Russell, S. W. (1982) *Prostaglandins 24*, 763.
Test, S. T., Lampert, M. B., Ossanna, P. J., Thoene, J. G., & Weiss, S. J. (1984) *J. Clin. Invest. 74*, 1341.
Tsan, M. F., Newman, B., & McIntyre, P. A. (1976) *Br. J. Haematol. 33*, 189.
Unkeless, J. (1977) *J. Exp. Med. 145*, 931.
Young, J. D. E., Unkeless, J. C., Young, T. M., Maro, A., & Cohn, Z. (1983) *Nature (London) 306*, 186.